G Model
CATTOD-9948; No. of Pages 8
ARTICLE IN PRESS
Catalysis Today xxx (2016) xxx–xxx
Contents lists available at ScienceDirect
Catalysis Today
journal homepage: www.elsevier.com/locate/cattod

Catalytic activity of $LiZr_2(PO_4)_3$ nasicon-type phosphates in ethanol conversion process in conventional and membrane reactors

Andrey B. Ilin*, Natalia V. Orekhova, Margarita M. Ermilova, Andrey B. Yaroslavtsev

A.V Topchiev Institute of Petrochemical Synthesis, Russian Academy of Sciences, Leninsky Pr. 29, Moscow, Russia

ARTICLE INFO

Article history:
Received 20 September 2015
Received in revised form
15 December 2015
Accepted 19 December 2015
Available online xxx

Keywords:
Nasicon catalyst
Membrane catalysis
Ethanol
Dehydration
Dehydrogenation

ABSTRACT

In this paper synthesis and catalytic properties of new catalysts based on double lithium-zirconium phosphate ($LiZr_2(PO_4)_3$) with monoclinic NASICON-type structure, doped by indium, niobium and molybdenum are discussed. The obtained samples with particle size of 50–300 nm were characterized by X-ray diffraction, scanning electron microscopy and X-ray microanalysis. The synthesized samples exhibit catalytic activity in the dehydration and dehydrogenation reactions of ethanol conversion. The main products were acetaldehyde, diethyl ether, hydrogen, C_2- and C_4-hydrocarbons. Indium- and molibdenum-doped samples were characterized by high activity in dehydrogenation processes, while niobium-doped was more active in dehydration processes. The highest selectivity in diethyl ether formation was achieved for $LiZr_2(PO_4)_3$ and Nb-doped samples (90 and 60% at 300 °C). The highest hydrogen yield (up to 60%) was obtained with the use of In-doped catalyst. $LiZr_2(PO_4)_3$ and Mo-doped samples are also noticeable for high C_4-hydrocarbons formation, selectivity to which reaches 60% at 390 °C. Use of a 100% hydrogen selective palladium-ruthenium alloy membrane increases hydrogen yield by 20%.

1. Introduction

Low-temperature fuel cells are the most promising alternative energy sources. For their implementation the new ways of hydrogen production based on renewable raw materials are developed. One of the most promising methods is bio-alcohols conversion. At the same time, alcohols can be used for obtaining a number of commercially important products, such as hydrocarbons, ethers, aldehydes, ketones, hydrogen, and so on. In this regard, new catalysts for the selective alcohols conversion into desired products need to be found.

Complex phosphates are considered as one of the promising types of catalysts for the alcohols conversion. Materials with NASICON (NA Super Ionic CONductor) structure type have general formula $A_xB_2(ZO_4)_3$, where A - is alkali or alkaline earth element, B - polyvalent element (Zr, Ti, Sc etc.), Z - phosphorus or silicon. Their structure is presented by edge-linked BO_6 octahedra and ZO_4 tetrahedra. A-cations are located in the cavities of this structure [1,2]

Interest in these compounds is determined primarily by their high ionic conductivity [3–5], which is achieved due to presence of conduction channels in their structure [2]. Other advantages of the NASICON-type compounds are high chemical, thermal and radiation stability. The variability of structure allows both iso- and heterovalent doping [6,7]. This defines a wide range of possible applications of these compounds [8–10] as lithium power sources [11,12], in fuel cells [13], in sensors [14–16], in radionuclide cleaning [17] and in catalysis [18–20].

The ability to heterovalent substitution is important for the catalytic applications, since it allows to vary the number and strength of acid (Brønsted and Lewis) and redox centers at the surface. Chemical and thermal stability allows to use catalysts based on such compounds in conditions in which the metal catalysts are degraded. Therefore, attempts to use these compounds as catalysts in alcohol conversion were made by the number of authors [21–28].

During the catalytic process certain products could be selectively separated or fed to the reaction mixture through membrane [29–31]. The main advantage of this method is the possibility of thermodynamic equilibrium shifting due to removal of product from reaction mixture. This is especially evident in reactions with hydrogen participation when membranes based on palladium alloys are used, because of their high hydrogen permeability [32–34]. Hydrogen, obtained in such reactors, requires no further purification due to high selectivity of such membranes. Nowadays many researches are devoted to carrying out catalytic processes in membrane reactors [35–39].

The aim of this work was to obtain the $LiZr_2(PO_4)_3$ NASICON-type phosphates with heterovalent substitution of the zirconium and phosphorus ions and their testing in the process of ethanol conversion. It was assumed that the substitution of some zirconium

* Corresponding author.
E-mail address: Novsel25@yandex.ru (A.B. Ilin).

http://dx.doi.org/10.1016/j.cattod.2015.12.017
0920-5861/

Please cite this article in press as: A.B. Ilin, et al., Catalytic activity of $LiZr_2(PO_4)_3$ nasicon-type phosphates in ethanol conversion process in conventional and membrane reactors, Catal. Today (2016), http://dx.doi.org/10.1016/j.cattod.2015.12.017

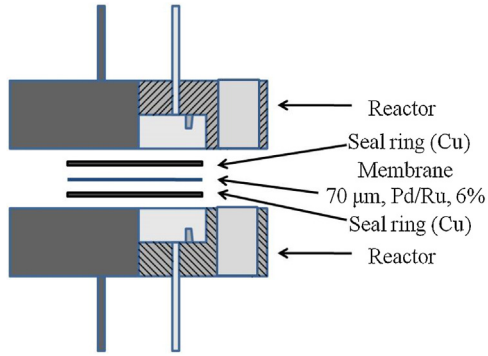

Fig. 1. The scheme of the used membrane reactor.

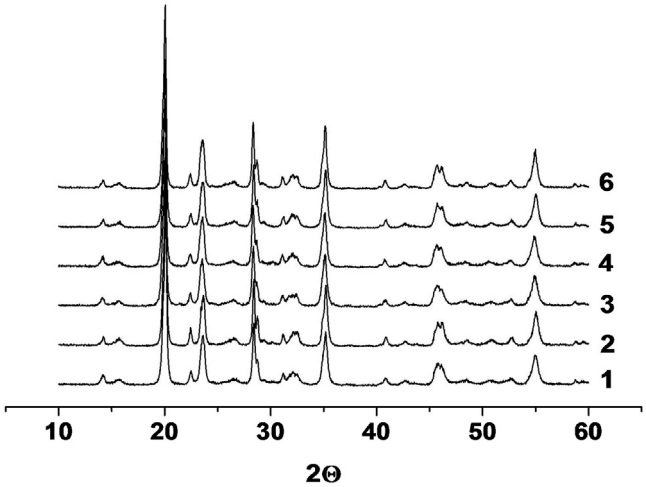

Fig. 2. X-ray patterns of the synthesized compounds. 1 - $LiZr_2(PO_4)_3$, 2 - $Li_{1.1}Zr_{1.9}In_{0.1}(PO_4)_3$, 3 - $Li_{0.9}Zr_{1.9}Nb_{0.1}(PO_4)_3$, 4 - $Li_{0.9}Zr_2P_{2.9}Mo_{0.1}O_{12}$, 5 - $LiZr_{1.8}In_{0.1}Nb_{0.1}(PO_4)_3$, 6 - $Li_{0.9}Zr_{1.8}In_{0.1}Nb_{0.1}P_{2.9}Mo_{0.1}O_{12}$.

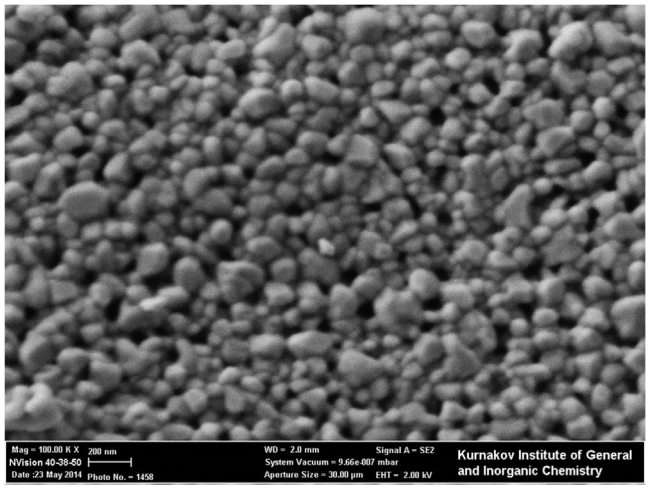

Fig. 3. A micrograph of a sample with composition $Li_{0.9}Zr_{1.8}In_{0.1}Nb_{0.1}P_{2.9}Mo_{0.1}O_{12}$.

ions on indium or niobium will change the acid-base properties of catalysts and their activity in dehydration processes. At the same time, replacement of the phosphorus on molybdenum will make them active in redox dehydrogenation processes.

The doped lithium-zirconium phosphate with NASICON structure can have catalytic activity in dehydrogenation and dehydration processes. It was assumed that a Pd-based membrane allows to extract hydrogen from the reaction mixture and displace the reaction equilibrium. For this purpose the obtained catalysts were investigated in the membrane reactor with Pd-Ru membrane. Advantages of this rector and membrane properties were discussed also.

2. Experimental

In this work the synthesis of the following compounds was carried out: $LiZr_2(PO_4)_3$, $Li_{1\pm0.1}Zr_{1.9}M_{0.1}(PO_4)_3$ (M = In and Nb), $LiZr_{1.8}In_{0.1}Nb_{0.1}(PO_4)_3$, $Li_{0.9}Zr_2P_{2.9}Mo_{0.1}O_{12}$ and $Li_{0.9}Zr_{1.8}In_{0.1}Nb_{0.1}P_{2.9}Mo_{0.1}O_{12}$, referred to below as LZP, LZInP, LZNbP, LZInNbP, LZPMo and LZInNbPMo, respectively. The synthesis was performed according to the Pechini method [28,40–43]. For this purpose a corundum crucible was used. $ZrOCl_2$ * $8H_2O$, citric acid, Li_2CO_3 and $NH_4H_2PO_4$ were successively dissolved in a mixture of ethylene glycol (2 ml) and deionized water (10 ml). The pH of the solution was quickly adjusted to 5.5 by adding concentrated ammonia solution to prevent precipitation of zirconium phosphate. The resulting solution was kept in the oven at 95 °C (24 h), 150 °C (24 h) and at 350 °C (4 h) for sequential removal of water and other gaseous components. After thoroughly grinding the resulting mixture was subjected to a final annealing at 750 °C for 10 h to form a NASICON phases. For LZInP synthesis In_2O_3 was dissolved in a minimum amount of hot concentrated nitric acid. This solution was added to ethylene glycol and deionized water first. $NbCl_5$ dissolved in the concentrated hydrochloric acid was used as the niobium source for LZNbP. The mixture of $NH_4H_2PO_4$ with $(NH_4)_6Mo_7O_{24}$ was used instead of $NH_4H_2PO_4$ for LZPMo synthesis. The samples, simultaneously doped with several elements, were obtained similarly.

X-ray diffraction (XRD) of samples was performed using X-ray diffractometer Rigaku D/Max-2200 ($CuK_{\alpha1}$ radiation), for spectra processing and qualitative analysis the Rigaku Application Data Processing software package was used. The particle size (coherent scattering region) was estimated on the base of the X-ray diffraction line broadening with the use of Scherrer equation:

$$d = \frac{k \times \lambda}{(B - b) \times \cos\theta} \quad (1)$$

where k = 0.89–Scherrer constant, λ = 1.5406 Å - the wavelength of the radiation used, B - the half-width at half-maximum of peak (2θ), b - the instrumental broadening (2θ), θ - the angle of the peak position. LaB_6 powder (Standard Reference Material® 660a) was used as the standard for determining the instrumental broadening.

The specific surface area was determined by the BET method with the use of Micromeritics ASAP 2020. The analysis was carried out in the relative pressures (p/p_o) area 0.01–0.99.

The micrographs of the samples were obtained by a scanning electron microscope (SEM) Carl Zeiss NVision 40 with an attachment for X-ray microanalysis. The accelerating voltage was 1 kV.

Catalytic properties were investigated in a conventional flow-type quartz tube reactor in the helium or argon stream with further identification of reaction products by chromatograph Crystallux–4000 M with thermal conductivity detector, columns HayeSep T 60/80 mesh (2 m, 150 °C, 30 cm^3/min, He), SKT–6 (2 m, 150 °C, 30 cm^3/min, He), Mole Seive 5 A (2 m, 25 °C, 30 cm^3/min, Ar). For these experiments, the 0.3 g of catalyst was mixed with milled quartz (d = 250–500 μm) and placed in the reactor with a 6 mm internal diameter so that the catalyst layer was 17 cm in length. To create the desired concentration of ethanol vapor, the carrier gas was passed at a volumetric flow rate of 20 cm^3/min through a bubbler with ethanol at 11 °C.

The scheme of the used membrane reactor is shown on Fig. 1. Palladium-ruthenium alloy foil (ruthenium proportion 6 mass%) tightened between two copper seal rings was used as a membrane with a thickness of 70 micron and active area of 7 cm^2. 0.3 g of

Table 1
The specific surface area and particle size characteristics of the synthesized compounds, estimated by different techniques.

Composition	Specific surface area, m^2/g	Particle size, nm	The average particle size estimated from the surface area, nm
$LiZr_2(PO_4)_3$	16 ± 1	49 ± 2	87
$Li_{1.1}Zr_{1.9}In_{0.1}(PO_4)_3$	11 ± 1	81 ± 4	174
$Li_{0.9}Zr_{1.9}Nb_{0.1}(PO_4)_3$	12 ± 1	73 ± 4	157
$Li_{0.9}Zr_2P_{2.9}Mo_{0.1}O_{12}$	20 ± 1	40 ± 2	94
$LiZr_{1.8}In_{0.1}Nb_{0.1}(PO_4)_3$	25 ± 1	51 ± 2	74
$Li_{0.9}Zr_{1.8}In_{0.1}Nb_{0.1}P_{2.9}Mo_{0.1}O_{12}$	8.0 ± 0.8	55 ± 3	229

catalyst mixed with 2.2 g of silica (fraction 250–500 μm) was placed into the bottom part of the reactor. Two flows of the carrier gas were passed at a volumetric flow rate of 20 cm^3/min in each part. The bottom flow was saturated with ethanol. In the experiment with an impermeable foil a stainless steel Plate 1 mm in thickness was used.

Acidity of catalysts was measured by thermoprogrammed desorption of NH_3 with the use of sorption analyzer USGA-101. 0.1–0.2 g of the sample was calcined at 550 °C in dry helium and then cooled down to 60 °C. NH_3 adsorption was carried out at 60 °C for 30 min using the NH_3/N_2 (1:1) mixture. Then the temperature was increased to 100 °C in order to remove physically-adsorbed NH_3. The final measurements were carried out in 60–800 °C temperature range in dry helium flow (30 ml/min) with heating speed of 8°/min.

The conversion (X), selectivity (S), yield (Y) of the samples were determined using the following formulas:

$$X = \frac{\varphi_0 - \varphi_1}{\varphi_0} \times 100\% \quad (2),$$

$$S = \frac{\varphi_i}{\varphi_0 - \varphi_1} \times 100\% \quad (3),$$

$$Y = \frac{\varphi_i}{\varphi_0 - \varphi_1} \quad (4),$$

where φ_0 and φ_1 are the initial and final volume fractions of alcohol, respectively; φ_i is the part of alcohol consumed to form product i.

Permeation rate was calculated as volume of hydrogen in cm^3, passed through 1 cm^2 of membrane per minute. The productivity of the samples was calculated as the amount of product (in millimoles) formed per one gram of catalyst per hour.

3. Results and discussion

3.1. The structure of the catalysts

According to X-ray phase analysis, all samples synthesized are single phase with monoclinic NASICON structure (Fig. 2). The calculated particle size, estimated with the use of X-ray diffraction line broadening, ranged from 50 to 80 nm (see Table 1). According to the SEM data their size consist 50–200 nm (Fig. 3).

The specific surface area of the catalysts synthesized lies in the range of 8–25 m^2/g (Table 1). The average particle size calculated from these data exceeds the value obtained from X-ray diffraction line broadening no less than 2 times (see Table 1). Along with the SEM data this allows us to conclude that a significant fraction of particles are aggregated. The indium and niobium doping leads to the increase of particle size and the decrease in samples specific surface area.

3.2. Catalytic transformation of ethanol in a quartz tube flow-type reactor

Catalytic tests carried out in the conventional flow-type tube quartz reactor showed that all synthesized samples exhibit activity in the dehydration and dehydrogenation reactions of ethanol. The blank experiments, which were carried out only with quartz particles (SiO_2, 250–500 μm) allow us to conclude that the alcohol conversion is catalyzed only by the synthesized phosphates (Fig. 4). The main products of the processes are diethyl ether, acetaldehyde, hydrogen, C_2-hydrocarbons (ethylene and ethane, formed by the hydrogenation of ethylene by hydrogen during the reaction) and C_4-hydrocarbons. CO, CO_2 and CH_4 formation was observed also, but their quantities were rather small compared to the main products.

The sample with composition of $LiZr_2(PO_4)_3$ is the most active in the formation of C_2- and C_4-hydrocarbons and diethyl ether. It shows the maximum ether yield, which reaches of 50% of all other

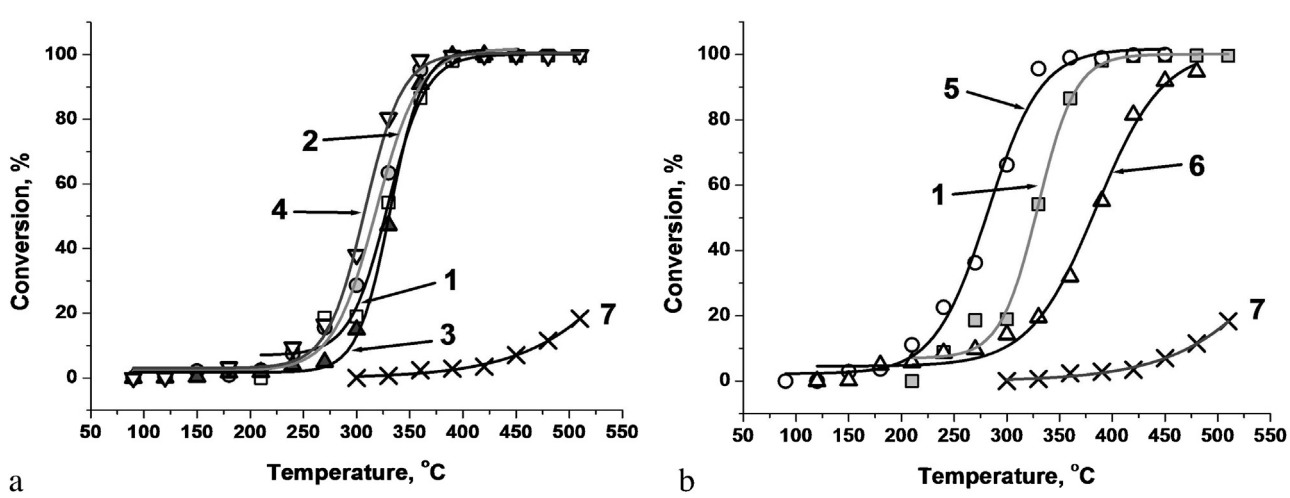

Fig. 4. The dependence of ethanol conversion versus temperature for catalysts with composition $LiZr_2(PO_4)_3$ (1), $Li_{1.1}Zr_{1.9}In_{0.1}(PO_4)_3$ (2), $Li_{0.9}Zr_{1.9}Nb_{0.1}(PO_4)_3$ (3), $LiZr_{1.8}In_{0.1}Nb_{0.1}(PO_4)_3$ (4), $Li_{0.9}Zr_2P_{2.9}Mo_{0.1}O_{12}$ (5), $Li_{0.9}Zr_{1.8}In_{0.1}Nb_{0.1}P_{2.9}Mo_{0.1}O_{12}$ (6), SiO_2 blank test (7).

Please cite this article in press as: A.B. Ilin, et al., Catalytic activity of $LiZr_2(PO_4)_3$ nasicon-type phosphates in ethanol conversion process in conventional and membrane reactors, Catal. Today (2016), http://dx.doi.org/10.1016/j.cattod.2015.12.017

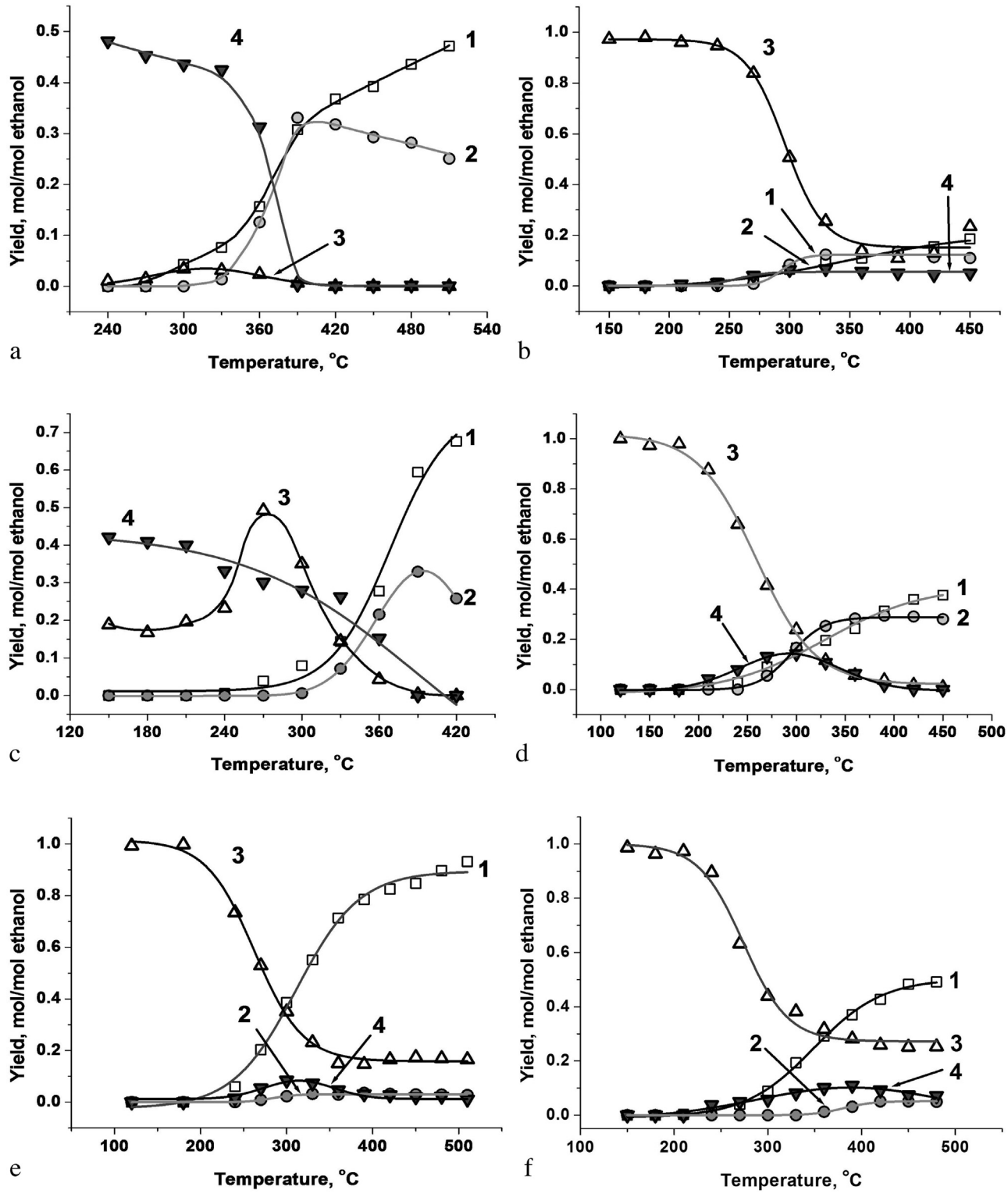

Fig. 5. Yield of C_2-hydrocarbons (1), C_4-hydrocarbons (2), acetaldehyde (3), diethyl ether (4) for the catalysts with composition $LiZr_2(PO_4)_3$ (a), $Li_{1.1}Zr_{1.9}In_{0.1}(PO_4)_3$, (b), $Li_{0.9}Zr_{1.9}Nb_{0.1}(PO_4)_3$ (c), $Li_{0.9}Zr_2P_{2.9}Mo_{0.1}O_{12}$ (d), $LiZr_{1.8}In_{0.1}Nb_{0.1}(PO_4)_3$ (e), $Li_{0.9}Zr_{1.8}In_{0.1}Nb_{0.1}P_{2.9}Mo_{0.1}O_{12}$ (f).

products (Fig. 5a). Nb doping results in enhanced dehydration properties and causes the increase in the ethylene yield, which may be associated with an increasing of the acidity of active sites due to the higher PO_4^{3-} groups polarization by Nb^{5+} ions. The doping by indium contrary leads to suppression of acid activity. At the same time doping by indium and molybdenum increases the dehydrogenation properties (yield of acetaldehyde). In the case of indium, this result can be considered quite surprising since it has only two stable oxidation states (0 and +3). However, it is known that stability of some monovalent indium compounds increases with rise of a temperature.

For samples doped with several elements simultaneously ethylene is the main product. It is the product of a monomolecular dehydration reaction:

$$C_2H_5OH \rightarrow C_2H_4 + H_2O,\ \Delta H^0_{298} = +28,99\ \text{kJ/mol} \quad (5)$$

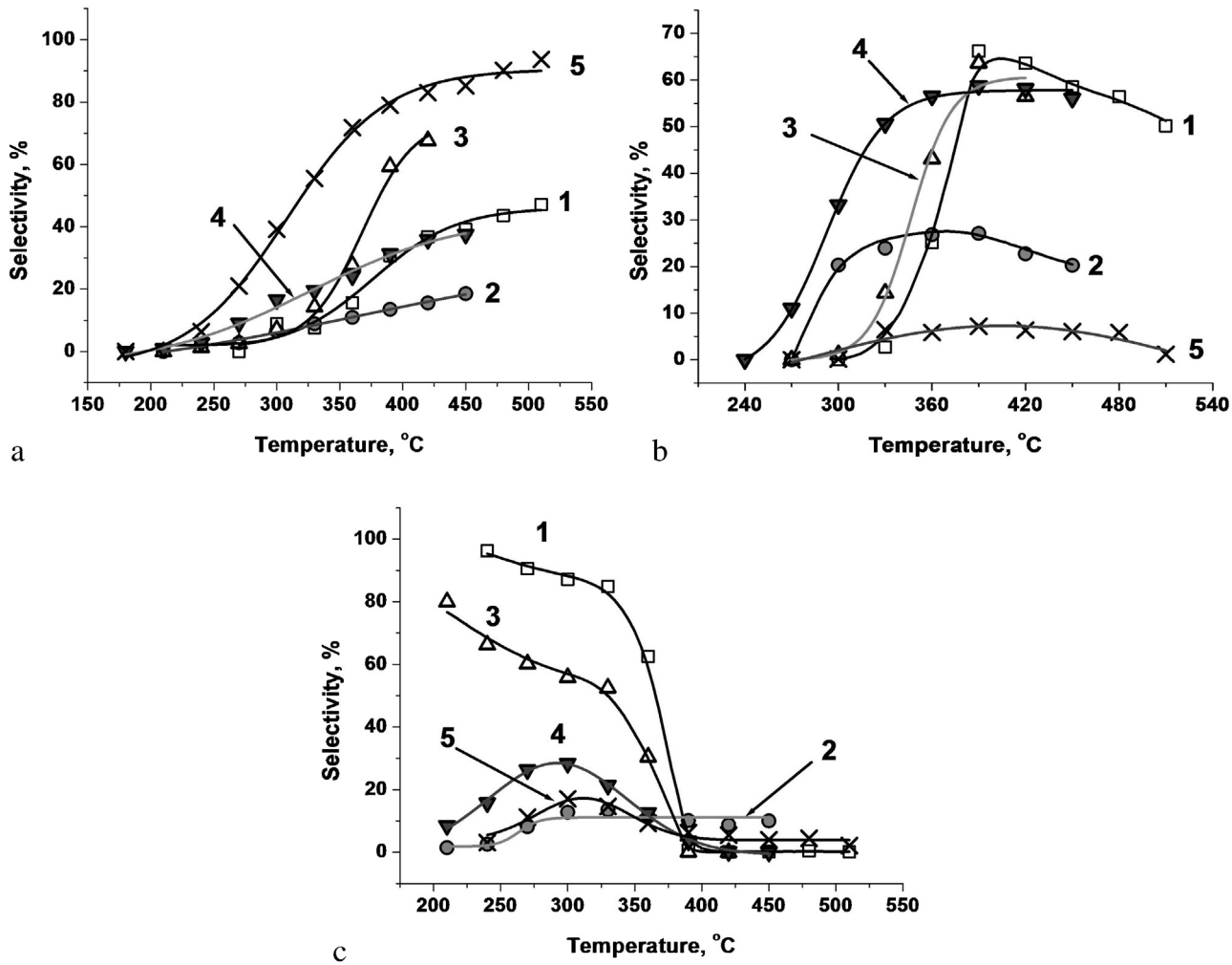

Fig. 6. The temperature dependence of selectivity to C_2-hydrocarbons (a), C_4-hydrocarbons (b), diethyl ether (c) for catalysts with composition $LiZr_2(PO_4)_3$ (1), $Li_{1.1}Zr_{1.9}In_{0.1}(PO_4)_3$ (2), $Li_{0.9}Zr_{1.9}Nb_{0.1}(PO_4)_3$ (3), $Li_{0.9}Zr_2P_{2.9}Mo_{0.1}O_{12}$ (4), $LiZr_{1.8}In_{0.1}Nb_{0.1}(PO_4)_3$ (5).

At first glance, it is similar to the diethyl ether formation reaction. But last reaction requires the simultaneous participation of two ethanol molecules. It should be ensured by the close location of the two centers with the dehydrogenation activity. In samples containing both niobium and indium, activity of some dehydrating centers increases and decreases for others. So the probability of close location of two active sites decreases. Therefore, despite the high activity in reactions of ethylene formation, their activity in ether formation is suppressed.

For the formation of C_4-hydrocarbons the simultaneous presence of centers active in dehydration and dehydrogenation is required. This reaction proceeds most active for the undoped and doped by molybdenum samples. At the same time it is interesting that in $Li_{0.9}Zr_{1.8}In_{0.1}Nb_{0.1}P_{2.9}Mo_{0.1}O_{12}$, in which both types of centers must be present, rate of this reaction is very small. It can be explained by the positive charge of centers containing molybdenum and niobium, which occupied phosphorus and zirconium positions respectively. Meanwhile indium ions located in zirconium positions, in contrast, have a negative charge. Therefore, the centers doped by molybdenum and indium have a tendency to association, niobium and molybdenum—to repulsion. This makes it unlikely location of the two centers having enhanced activity in the dehydration and dehydrogenation reactions in $Li_{0.9}Zr_{1.8}In_{0.1}Nb_{0.1}P_{2.9}Mo_{0.1}O_{12}$.

Highest selectivity (close to 100%) is achieved at low temperatures for all the catalysts (Fig. 6). For $LiZr_2(PO_4)_3$ and $Li_{0.9}Zr_{1.9}Nb_{0.1}(PO_4)_3$ catalysts dimethyl ether is the main product and acetaldehyde dominates in all other cases. However, at lower temperatures the selectivity is not as important as at higher, since the reaction rate and conversion is very low. For $Li_{0.9}Zr_{1.9}Nb_{0.1}(PO_4)_3$ high selectivity to diethyl ether (60%) persists up to 300 °C. For all other catalysts several products are formed simultaneously at higher temperatures. An exception is $LiZr_{1.8}In_{0.1}Nb_{0.1}(PO_4)_3$, for which at above 350 °C the ethylene is the dominant product with selectivity is more than 90%. And valuable is the fact that for $LiZr_2(PO_4)_3$ and $Li_{0.9}Zr_2P_{2.9}Mo_{0.1}O_{12}$ at high temperatures C_4-hydrocarbons are formed with selectivity up to 60%. It should be noted also that the molybdenum doping reduces the temperature of the reaction on 60 °C.

The $LiZr_2(PO_4)_3$ and Nb-doped samples have the highest concentration of high acidity centers (Fig. 7a,c). At lower temperatures these catalysts showed the highest selectivity in diethyl ether formation (curves 1, 3 of Fig. 6 c). In the high temperature range all acid sites take part in the reaction route, thus, a sample with higher specific surface area posses higher dehydration properties. This is most typical for $LiZr_{1.8}In_{0.1}Nb_{0.1}(PO_4)_3$ sample with 25 m^2/g of specific surface area and high concentration of acid centers. The selectivity of ethylene formation reaches 80% at 400 °C for this sample (curve 5 of Fig. 6a).

The indium-doped sample shows the highest activity in hydrogen formation (Fig. 8a). Most likely, this is due to the fact that the function of dehydration in the sample is suppressed, while dehy-

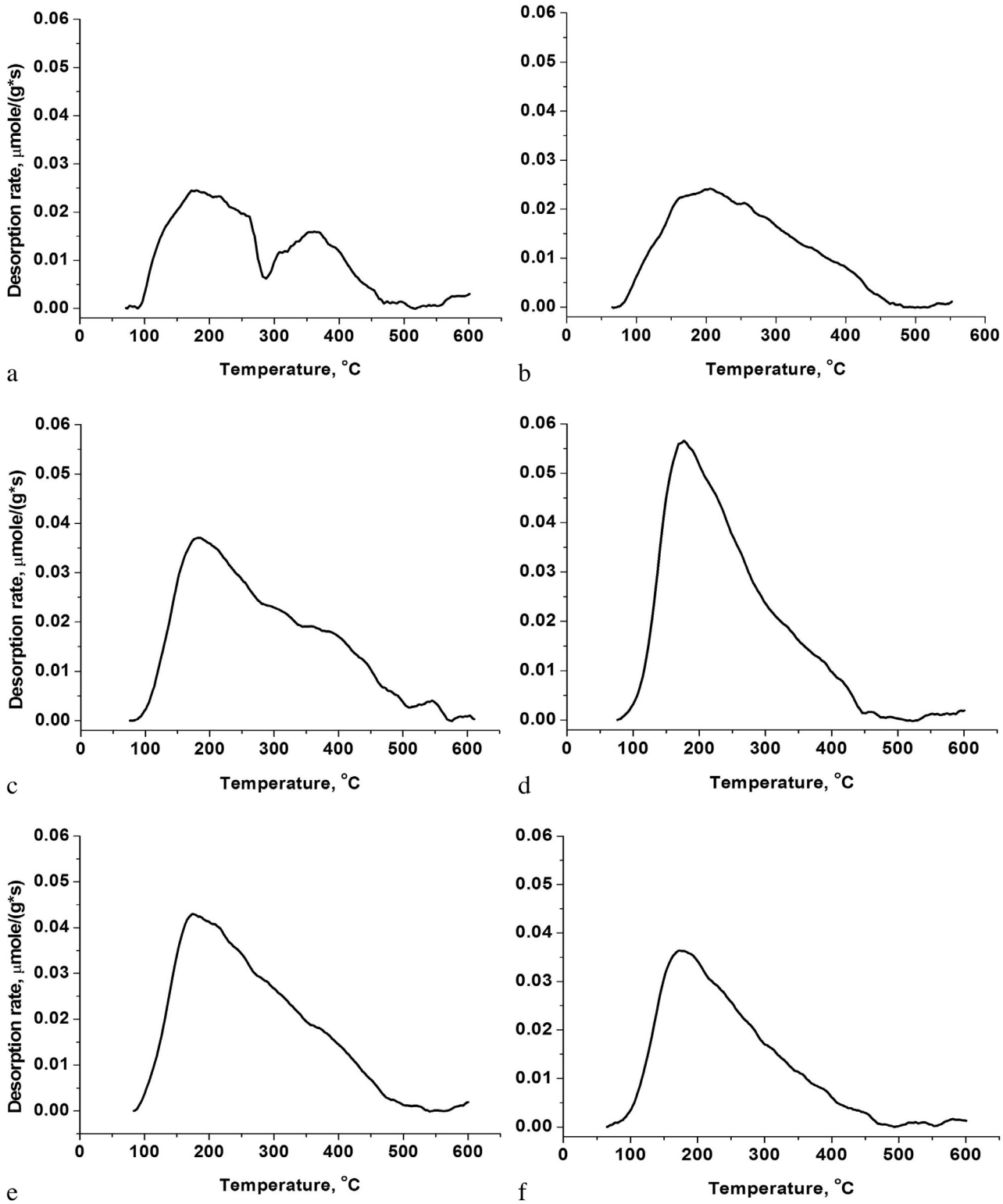

Fig. 7. Rates of NH_3 desorption for the samples with composition $LiZr_2(PO_4)_3$ (a), $Li_{1.1}Zr_{1.9}In_{0.1}(PO_4)_3$ (b), $Li_{0.9}Zr_{1.9}Nb_{0.1}(PO_4)_3$ (c), $Li_{0.9}Zr_2P_{2.9}Mo_{0.1}O_{12}$ (d), $LiZr_{1.8}In_{0.1}Nb_{0.1}(PO_4)_3$ (e), $Li_{0.9}Zr_{1.8}In_{0.1}Nb_{0.1}P_{2.9}Mo_{0.1}O_{12}$ (f).

drogenation function increases. In $Li_{0.9}Zr_2P_{2.9}Mo_{0.1}O_{12}$ not only dehydrogenation activity enhanced, but the activity of the dehydration increased also. At the same time, at low temperatures, when the dehydrogenation rate is low, it is possible that a part of the hydrogen produced is consumed by the partial molybdenum reduction. In this regard indium-doped catalyst was selected for the experiments in a membrane reactor

3.3. Transformation of the ethanol in the membrane reactor

Compared to the experiments with the impermeable stainless steel foil, the reactor with palladium-ruthenium alloy as a membrane, $Li_{1.1}Zr_{1.9}In_{0.1}(PO_4)_3$ catalyst increases the hydrogen production by 20% (Fig. 9a). Increase in the ethanol conversion is also observed (Fig. 9b). These effects are attributed to the shifting of

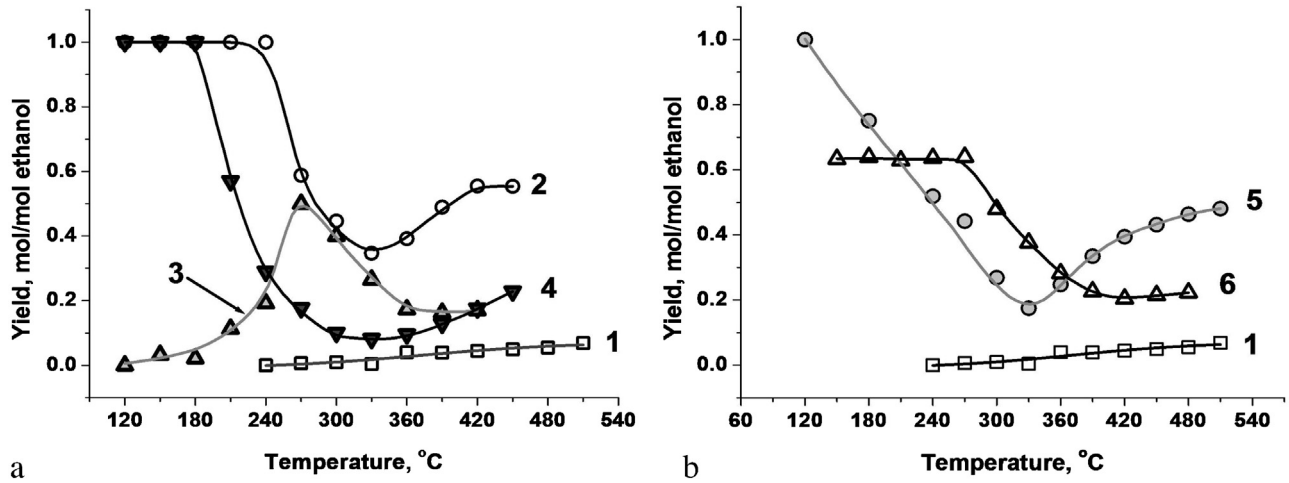

Fig. 8. Hydrogen yield for the catalysts with composition $LiZr_2(PO_4)_3$ (1), $Li_{1.1}Zr_{1.9}In_{0.1}(PO_4)_3$ (2), $Li_{0.9}Zr_{1.9}Nb_{0.1}(PO_4)_3$ (3), $Li_{0.9}Zr_2P_{2.9}Mo_{0.1}O_{12}$ (4) - (a), and $LiZr_2(PO_4)_3$ (1), $LiZr_{1.8}In_{0.1}Nb_{0.1}(PO_4)_3$ (5), $Li_{0.9}Zr_{1.8}In_{0.1}Nb_{0.1}P_{2.9}Mo_{0.1}O_{12}$ (6) - (b).

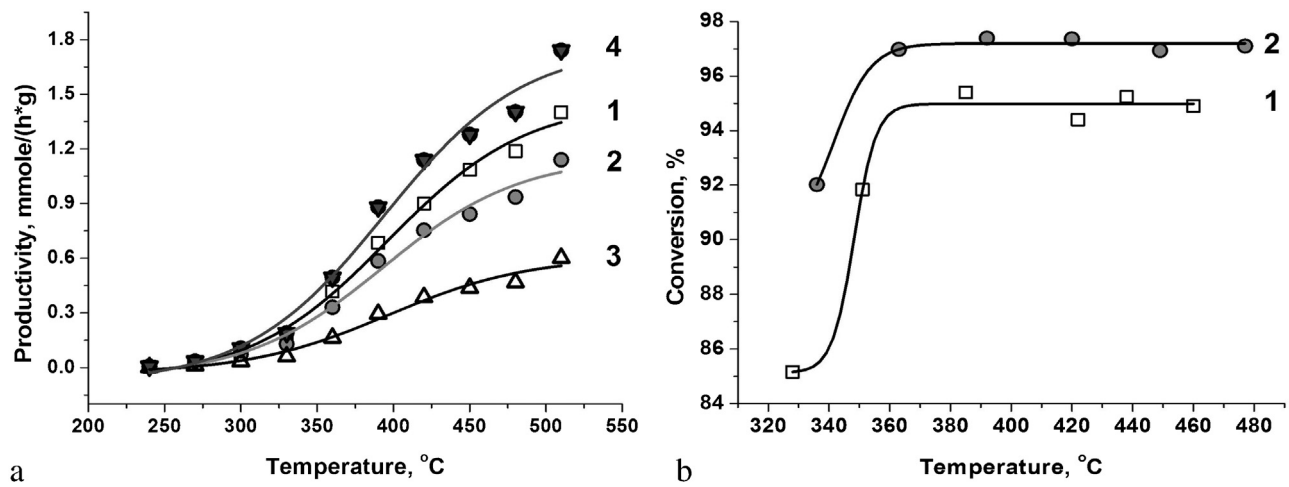

Fig. 9. Hydrogen productivity in experiments with impermeable foil (1) and the membrane (2, 3, 4), where (2) - retentate, (3) - permeate, (4) - the sum of the permeate and retentate - (a) and ethanol conversion in membrane reactor with impermeable foil (1) and the membrane (2) - (b).

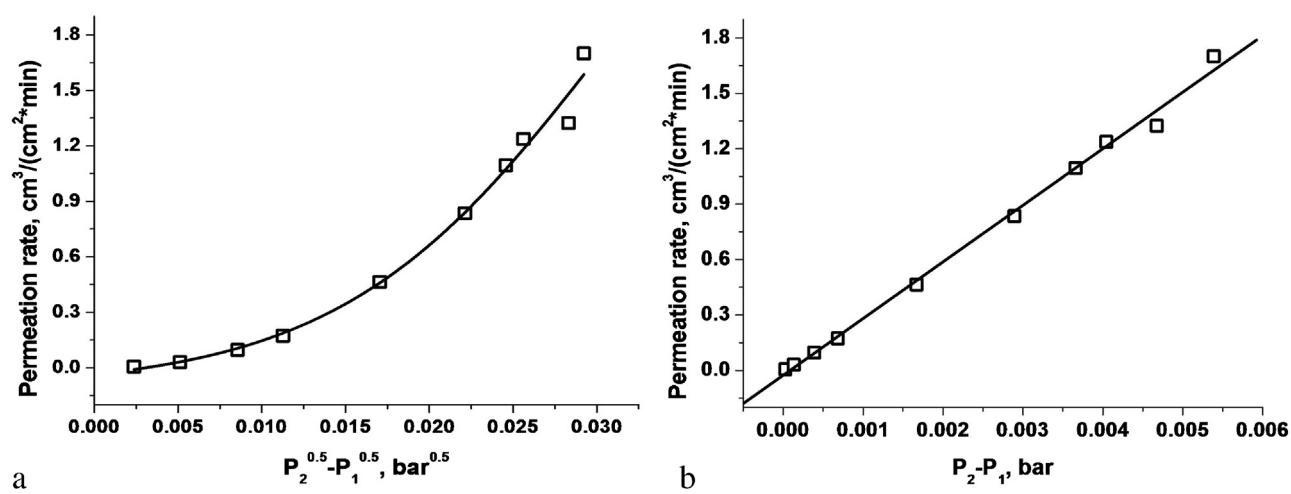

Fig. 10. The dependence of hydrogen permeation on $(P_2^{0,5}-P_1^{0,5})$ - (a) and (P_2-P_1) - (b).

Please cite this article in press as: A.B. Ilin, et al., Catalytic activity of $LiZr_2(PO_4)_3$ nasicon-type phosphates in ethanol conversion process in conventional and membrane reactors, Catal. Today (2016), http://dx.doi.org/10.1016/j.cattod.2015.12.017

the thermodynamic equilibrium due to removal of hydrogen from the reaction mixture in the membrane reactor.

The recovery rate of hydrogen does not change with the temperature increasing and its average mean is about 35%. The hydrogen productivity increases significantly with increase in hydrogen conversion. The permeate contains hydrogen without any other impurities.

Hydrogen permeates through membrane via a solution-diffusion mechanism [44]. Thus, the hydrogen transfer is affected by its diffusion through the bulk metal and hydrogen pressure difference in retentate and permeate zones. Hydrogen permeation (J) can be described by the equation:

$$J = \frac{P \times (p_2^n - p_1^n)}{l} \quad (6)$$

where P is hydrogen permeability constant, l is a membrane thickness, p_1 and p_2 are the partial hydrogen pressures in the permeate and retentate zones respectively, n is a constant depending on the diffusion mechanism.

If the atomic hydrogen diffusion in the membrane bulk is the rate-controlling stage, n value should be equal to 0.5 because of equilibrium between molecular hydrogen in gaseous phase and dissolved atomic hydrogen. (Sieverts law [45]). But Sieverts law is not complied in our case (Fig. 10a). The dependence becomes linear for n value equal to 1 (Fig. 10b). This means that the rate-controlling stage involves hydrogen in molecular form only. It is reasonable to suppose that it took place in retentate zone because of the competitive adsorption of other reaction products and hydrogen on membrane surface [46–48]. In the permeate zone only hydrogen and sweep gas were found, so the competitive adsorption in this zone cannot occur. Also the experiments with different carrier gases (Ar and He) were carried out and it was established that even helium doesn't pass through membrane which means that there are no holes in membrane through which molecular hydrogen can pass in permeate zone.

Within an hour the hydrogen stream in the membrane reactor decreases by 40% due to the catalyst carbonization. Calcination in an air stream allows to regenerate the catalyst and to improve its activity up to its original level.

4. Conclusion

The single-phase catalysts were obtained based on double lithium-zirconium phosphate with NASICON-type structure $LiZr_2(PO_4)_3$ doped by In, Nb, and Mo, with a particle size less than 200 nm. All samples exhibit activity in the ethanol dehydration and dehydrogenation processes. The main products are the C_2- and C_4-hydrocarbons, diethyl ether, acetaldehyde and hydrogen. It has been shown that the doping by indium increases the yield of acetaldehyde and hydrogen, doping by niobium - diethyl ether and ethylene. Molybdenum incorporation increases the catalyst activity in the ethanol dehydrogenation rate and reduces the temperature of the reaction on 60 °C. It is worth mentioned that C_4-hydrocarbons are formed on $LiZr_2(PO_4)_3$ and $Li_{0.9}Zr_2P_{2.9}Mo_{0.1}O_{12}$ catalysts with selectivity up to 60% at high temperatures.

Carrying out the process in a membrane reactor leads to the increase in the hydrogen yield due to the thermodynamic equilibrium shift and increase in the ethanol conversion.

Acknowledgement

This work was supported by the Russian Foundation for Basic Research, grant no. 13-08-00660.

References

[1] L.O. Hagman, P. Kierkegaard, Acta Chem. Scand. 22 (1968) 1822.
[2] H. Kohhler, H. Schulz, Mat. Res. Bull. 20 (1985) 1461–1471.
[3] Hong H.Y.-P, Crystal structures and crystal chemistry in the system $Na_{1+x}Zr_2Si_xP_{3-x}O_{12}$//, Mater. Res. Bull. 11 (2) (1976) 173–182.
[4] S. Roy, P.P. Kumar, Solid State Ionics 253 (2013) 217–222.
[5] P. Zhang, H. Wang, Q. Si, M. Matsui, Y. Takeda, O. Yamamoto, N. Imanishi, Solid State Ionics 272 (2015) 101–106.
[6] I.A. Stenina, A.B. Yaroslavtsev, Z. Neorg. Khim. 51 (2006) 95-114.
[7] V.I. Petkov, Rus. Chem. Rev. 7 (2012) 606–637.
[8] G.-A. Nazri, G. Pistoia, Lithium Batteries: Science and Technology, Kluwer Academic Publishers, Boston, Dordrecht, New York, London, 2004, pp. 708.
[9] D. Morgan, G. Ceder, M.Y. Saidi, J. Barker, J. Swoyer, H. Huang, G. Adamson, J. Pow. Sour. 119–121 (2003) 755–759.
[10] M.Y. Saidi, J. Baker, H. Huang, J.L. Swoyer, G. Adamson, J. Pow. Sour. 119–121 (2003) 266–272.
[11] A.D. Robertson, A.R. West, A.G. Ritchie, Solid State Ionics. 104 (1997) 1–11.
[12] S.R.S. Prabaharan, S. Ramesh, M.S. Michael, K.M. Begam, Mat. Chem. Phys. 87 2–3 (2004) 318–326.
[13] G. Pasciak, K. Prociow, W. Mielcarek, B. Gornicka, B. Mazurek, J. Europ. Ceram. Soc. 21 (10–11) (2001) 1867–1870.
[14] M. Cretin, P. Fabry, J. Eur. Ceram. Soc. 19 (1999) 2931–2940.
[15] T. Kida, H. Kawate, K. Shimanoe, N. Miura, N. Yamazoe, Solid State Ionics. 136–137 (2000) 647–653.
[16] G. Paściak, W. Mielcarek, K. Prociów, J. Warycha, Ceram. Int. 40 (8B) (2014) 12783–12787.
[17] R.D. Ambashta, M.E.T. Sillanpää, J. Environ. Radioact. 105 (2012) 76–84.
[18] P. Agaskar, R. Grasselli, D. Buttrey, B. White, Stud. Surf. Sci. Catal. 110 (1997) 219.
[19] A.I. Orlova, V.L. Pet'kov, S.T. Gul'yanova, M.M. Ermilova, S.L. Ienealem, O.K. Samuilova, T.K. Chekhlova, V.M. Gryaznov, Russ. J. Phys. Chem. A. 73 (11) (1999) 1767–1769.
[20] I.I. Mikhalenko, E.I. Povarova, A.I. Pylinina, Nauchn. Vedom. Belarus. Gos. Univ. Ser.: Mat. Fiz. 27 (130) (2012) 169–174, 11.
[21] M.A. Aramendia, V. Borau, J.M. Marinas, F.J. Romero, Chem. Lett. (1994) 1361–1364.
[22] A. Serghini, R. Brochu, M. Ziyad, J. Vedrine, J. Chem. Soc. Faraday Trans. 87 (15) (1991) 2487–2493.
[23] Y. Brik, M. Kacimi, F. Bozon-Verduraz, M. Ziyad, Microporous Mesoporous Mater. 43 (2001) 103–112.
[24] A.B. Il'in, S.A. Novikova, M.V. Sukhanov, M.M. Ermilova, N.V. Orekhova, A.B. Yaroslavtsev, Inorg. Mater. 48 4 (2012) 397–401.
[25] E.I. Povarova, A.I. Pylinina, I.I. Mikhalenko, Russ. J. Phys. Chem. A 86 (6) (2012) 935–941.
[26] A.I. Pylinina, I.I. Mikhalenko, Mendeleev Commun. 22 (2012) 150–151.
[27] A.I. Pylinina, I.I. Mikhalenko, Russ. J. Phys. Chem. A. 87 (3) (2013) 372–375.
[28] A.B. Il'in, M.M. Ermilova, N.V. Orekhova, A.B. Yaroslavtsev, Inorg. Mater. 51 (7) (2015) 778–784.
[29] I.F.J. Vankelecom, K.A.L. Vereruysse, P.E. Neys, et al., Top. Catal. 5 (1998) 125–132.
[30] V. Diakov, A. Varma, Chem. Eng. Sci. 57 (2002) 1099–1105.
[31] R. Tesser, M.D. Serio, E. Santacesaria, Catal. Today 77 (2003) 325–333.
[32] A. Iulianelli, P. Ribeirinha, A. Mendes, A. Basile, Renew. Sustainable Energy Rev. 24 (2014) 355–368.
[33] A. Iulianelli, A. Basile, Catal. Sci. Technol. 1 (2011) 366–379.
[34] E. Yu, A.A. Mironova, M.M. Lytkina, M.N. Ermilova, L.M. Efimov, N.V. Zemtsov, G.P. Orekhova, G.N. Karpacheva, D.N. Bondarenko, A.B. Muraviev, Yaroslavtsev, Int. J. Hydrogen Energy 40 (2015) 3557–3565.
[35] B. Krishna, R. Nair, M.P. Harold, Chem. Eng. Sci. 61 (2006) 6616–6636.
[36] A. Basile, A. Parmaliana, S. Tosti, A. Iulianelli, F. Gallucci, C. Espro, J. Spooren, Catal. Today 137 (2008) 17–22.
[37] A. Iulianelli, S. Liguori, T. Longo, P. Pinacci, A. Basile, Int. J. Hydrogen Energy 35 (2010) 3170–3177.
[38] A. Iulianelli, A. Basile, Int J. Hydrogen Energy 35 (2010) 3159–3164.
[39] P.K. Seelam, S. Liguori, A. Iulianelli, P. Pinacci, V. Calabrò, M. Huuhtanen, R. Keiski, V. Piemonte, S. Tosti, M. De Falco, A. Basile, Catal. Today 219 (2012) 42–48.
[40] M.P. Pechini, US Patent 3.3306.97. 1967.
[41] M. Kakihana, M. Yoshimura, Bull. Chem. Soc. Jpn. 72 (1999) 1427–1443.
[42] C.R. Mariappan, C. Galven, M.-P. Crosnier-Lopez, F. Le Berre, O. Bohnke, J. Solid State Chem. 179 (2) (2006) 450–456.
[43] F. Ejehi, S.P.H. Marashi, M.R. Ghaani, D.F. Haghshenas, Ceram. Int. 38 (8) (2012) 6857–6863.
[44] F.A. Lewis, The Palladium Hydrogen System, Academic Press, London, 1967.
[45] A. Sieverts, W. Kumbhaar, Ber. Deut. Chem. Gas. 43 (1910) 893.
[46] M. Vandrucci, F. Borgognioni, A. Moriani, A. Santucci, S. Tosti, Hydrogen permeation through Pd–Ag membranes: surface effects and Sieverts' law, Int. J. Hydrogen Energy 38 (2013) 4144–4152.
[47] W.-H. Chen, M.-H. Hsia, Y.-L. Lin, C.-C. Yang, Appl. Energy 113 (2014) 41–50.
[48] A. Basile, Top. Catal. 51 (2008) 107–122.